Tellus (1983), *35B*, 31–39

An analysis of the surface production of sea-salt aerosols

By C. W. FAIRALL, *BDM Corporation, Naval Postgraduate School, Monterey, California 93940, U.S.A.*
K. L. DAVIDSON and G. E. SCHACHER, *Environmental Physics Group, Naval Postgraduate School, Monterey, California 93940, U.S.A.*

(Manuscript received December 22, 1981; in final form June 22, 1982)

ABSTRACT

The rate of production of sea water droplets by bubble bursting at the ocean surface is very difficult to measure directly. Laboratory simulations are also difficult. However, the surface flux can be inferred from measurements of the rate of change of aerosol densities and changes in the height of the marine boundary layer. Data from CEWCOM-78 have been analyzed to produce the aerosol surface flux volume spectrum from 0.8 to 15 μm radius at a wind speed of 9 m s^{-1}. Using this flux spectrum and equilibrium aerosol spectra from JASIN, flux spectra are calculated for wind speeds from 6 to 18 m s^{-1}.

1. Introduction

There are two components to aerosols in the marine boundary layer: (1) continental (background) and (2) locally generated sea-spray droplets (Barnhardt and Streete, 1970). The sea-spray droplets are generated primarily by the bursting of bubbles at the sea surface (Blanchard and Woodcock, 1975). The bubbles are produced by biological activity, chemical reaction and breaking waves (white caps). At wind speeds greater than about 3 meters per second, white caps are the primary contributor to the bursting bubbles. Thus, the sea surface is a continuous source of sea-salt aerosols in the marine boundary layer. These surface-produced aerosols can be characterized by a surface flux spectrum $F_s(r)$, which represents the volume of aerosol per particle radius interval produced per cm^2 of ocean surface each second as a function of aerosol particle radius. This quantity is a function of wind speed.

The continuous production of sea-salt aerosols is balanced by several removal mechanisms. One obvious mechanism is the loss of particles as they fall back to the surface. This settling under gravity is called "Stokes fallout" and is characterized by the Stokes velocity. The particles are transported vertically by turbulence in the marine boundary layer and maintained at a nearly uniform mixing ratio throughout the mixed layer. The growth of the height of the layer constitutes another loss mechanism called "entrainment" (Deardorff, 1976). The final major loss mechanism is "rainout" which occurs when the particles become condensation nuclei in the formation of clouds.

Given the surface flux spectrum and a parameterization of the removal mechanisms, one could predict evolutions of the aerosol density spectrum (Fairall *et al.*, 1982). Unfortunately, the surface flux spectrum is not known. However, we can reverse the process—that is, use parameterizations of the removal processes and evolutions of the aerosol spectrum—to obtain estimates of the surface flux spectrum. This paper describes the calculation of $F_s(r)$ from data taken by the NPS Environmental Physics Group during the Cooperative Experiment for West Coast Oceanography and Meteorology (CEWCOM-78) and the Joint Air-Sea Interaction Experiment (JASIN). Details about the experiments, equipment, measurements, and analysis are given by Schacher *et al.* (1981).

2. Aerosol spectrum

The first step to analyzing the evolution of the aerosol spectrum is to remove those variations due

0280-6509/83/010031-09$02.50/0

to changes in the ambient relative humidity. This is done by transforming each spectrum to a reference relative humidity (RH = 80% or a saturation ratio $S = 0.8$). We make the usual assumption that the particle radius at water vapor saturation ratio S is given by (Fitzgerald, 1975).

$$r_S = rg(S) \tag{1}$$

where r is the radius at a standardized saturation ratio $S = S_0 = 0.8$ and $g(S) = 0.81 \exp [0.066S/(1.058 - S)]$. This form for $g(S)$ is given by Hughes and Richter (1980). If we have a measured aerosol number density spectrum, $n'(r_S)$, then the transformed spectrum at the standard saturation ratio, $n(r)$, is:

$$dN/dr = n(r) = n'(rg(S))g(S) \tag{2}$$

Since we prefer to work with the volume spectrum $v(r) = 4/3\pi r^3 n(r)$, the corresponding relationship is:

$$dV/dr = v(r) = v'(rg(S))/g^2(S) \tag{3}$$

We now must separate the measured spectrum into its two basic components:

(1) the background continental aerosol of non-local origin, v_c, which is present above and within the marine layer; and

(2) the sea-salt aerosol locally generated at the sea surface, v_s, which is well-mixed throughout the marine layer (h is the height of the mixed layer). Note that the capital "S" in eq. (1) refers to saturation ratio while the small "s" here refers to sea salt. Thus, we assume:

$$v(r) = v_c(r) + v_s(r) \quad Z < h \tag{4a}$$

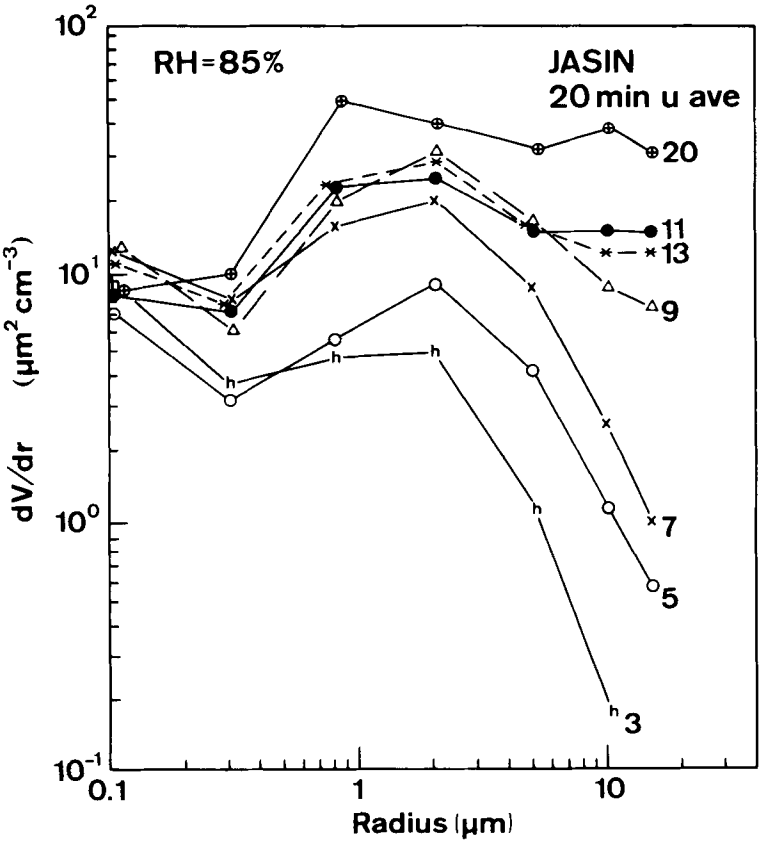

Fig. 1. Ensemble average total aerosol volume spectra from JASIN. The number to the right of the spectrum is the wind speed category in m/sec.

$$v(r) = v_c(r) \quad Z > h \tag{4b}$$

The continental aerosol component at standard saturation ratio is represented with a Junge type distribution

$$v_c(r) = A/r \tag{5}$$

where A is the continental coefficient at the standard saturation ratio. Since there is very little sea-salt volume production for $r < 0.3$ μm (Monahan *et al.*, 1982), we can use the small size range of the spectrum to calculate the continental coefficient ($A = rv(r)$). This is documented in Fig. 1 where ensemble averages of volume spectra indicated that $v(r)$ is essentially independent of wind speed at $r = 0.1$ μm. Although the sea may be a source of sea salt particles at $r \leq 0.1$ μm, these particles represent a very small fraction of particles from other sources. At low wind speeds, the $r = 0.1$ μm and $r = 0.3$ μm ensemble average spectra are described quite accurately by eq. (5). Certainly eq. (5) is an over simplification but since the continental component contributes very little for $r > 1$ μm, the exact details of the shape of the continental spectrum is probably unimportant here. The claim that A is an accurate index of continental influence is nicely validated by comparison with atmospheric Radon activity (Larson *et al.*, 1979) from CEWCOM-78 (Fig. 2). Note that A is at the standard saturation ratio: under ambient conditions one would observe $A' = Ag^3(S)$. Thus, the locally generated sea-salt component can be calculated using:

$$v_s(r) = v(r) - A/r \tag{6}$$

Eq. (6) is not very useful for estimating $v_s(r)$ for $r < 0.5$ μm since it represents the difference of two quantities of approximately the same magnitude.

The remainder of this paper will deal exclusively with the volume spectra transformed to standard humidity, $v_s(r)$, to simplify the notation with the understanding that v_s refers to the spectrum at RH = 80%, with radius, r, an implied variable.

The evolution of the aerosol spectrum in the well mixed marine boundary layer is described by the following equation (Fairall *et al.*, 1982).

$$h\, dv_s/dt = F_s - (W_e + W_k)v_s \tag{7}$$

(which is presented here without further discussion)

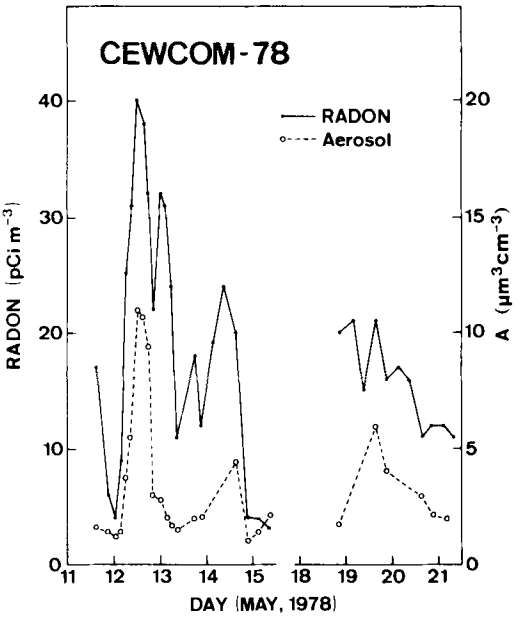

Fig. 2. Time series of atmospheric ^{222}Rn activity (solid line, Larsen, Kasemir and Bressan, 1979) and continental aerosol coefficient at the standard saturation ratio (dashed line), A.

where W_e is the entrainment velocity and W_k is the Stokes velocity (Wu, 1979)

$$W_k = 1.57 \times 10^{+8} \times (1 + 1.2(0.81/g(S))^3)r^2g^2(S) \tag{8a}$$

$$W_e = dh/dt - W \tag{8b}$$

where r is in m and W_k is in m s^{-1} and W is the mean vertical air motion due to synoptic scale weather (subsidence). In eq. (7) we have left out the cloud formation removal mechanism because it acts on a much longer time scale. We have also neglected coagulation because of the very low number densities (typically less than 100 cm^{-3}) of these particles. One assumption implicit in eq. (7) is that the convective mixing velocity, $W*$ (Kaimal *et al.*, 1976), is much larger than W_k. Since $W*$ is typically 1 m s^{-1} (Kaimal *et al.*, 1976; Markson *et al.*, 1981) while W_k is of the order of 0.1 m s^{-1} for the largest particles ($r = 15$ μm) considered here, the assumption is reasonable.

3. Flux spectrum analysis

The CEWCOM-78 data have been used to evaluate the surface flux term of eq. (7). Since the other terms of the expression were measured, one simply calculates F_s using a rearrangement of the terms. Thus the final expression for the flux calculation is,

$$F_s = h\,\mathrm{d}v_s/\mathrm{d}t + (W_e + W_k)v_s \qquad (9)$$

A period was chosen from CEWCOM-78 where all data were available, the synoptic conditions were fairly stable, the wind speed was reasonably constant and a good mixed layer was present (Table 1). There was a slowly decreasing continental influence indicative of steady NW winds (A in Table 1 and Fig. 2). The mixed layer depth, h, was of the order of 400 m, which is typical for this area. An acoustic sounder was used to monitor h continuously (h was also determined several times a day from standard radiosonde data).

Application of eq. (9) requires a value for the entrainment velocity. If the subsidence velocity is known, then W_e can be calculated from $\mathrm{d}h/\mathrm{d}t$ using eq. (8b). Since it is difficult to obtain W to 0.1 cm s^{-1} accuracy, it was decided to estimate W_e empirically from the evolution of the mixed layer temperature and water vapor density. This was accomplished by simulating the analysis period with a dynamic mixed layer model. After initializing the model with atmospheric parameters at the beginning of the period, the entrainment velocity was adjusted to yield best agreement with the temperature and water vapor density at the end of the period. The mean W_e for the period was 0.35 cm s^{-1}. This implies $W = -0.3$ cm s^{-1} for the first 8 h and $W = 0$ for the last 12 h.

The scatter and uncertainty of the aerosol and mixed layer depth measurements introduces certain trade-offs between averaging times and statistical validity. For short averaging times, the random scatter of the individual terms is considerable, leading to large variations in the time derivative terms. By increasing the averaging time to 4 h, random variations of F_s are significantly reduced compared to the mean of F_s. A time series of the individual terms of eq. (9) is shown in Fig. 3 for two different particle sizes. The average surface produc-

Table 1. *CEWCOM-78 meteorological and aerosol data for the time period analyzed for this report. The aerosol volume spectra density dV/dr is given at each radius, r, in μm. The height of the boundary layer was determined from an acoustic sounder*

Date	Time	U (m s^{-1})	RH (%)	h (m)	A	$r = 0.3$ (μm^2 cm^{-3})	$r = 0.8$	$r = 2$	$r = 5$	$r = 10$	$r = 15$
May 20	1130	7.4	89.4	420	7.8	15.1	12.5	9.79	2.26	0.80	0.43
May 20	1230	7.7	87.6	430	5.2	9.15	12.5	11.9	2.08	0.64	0.32
May 20	1330	8.2	86.4	430	4.5	8.39	11.9	12.2	2.91	1.11	0.62
May 20	1430	8.1	82.1	415	4.7	8.54	10.6	11.4	2.24	0.78	0.42
May 20	1530	8.3	80.9	437	4.0	7.96	12.0	11.2	1.26	0.29	0.12
May 20	1630	8.2	81.1	437	4.0	7.85	11.9	13.6	2.47	0.79	0.41
May 20	1730	9.0	82.5	443	3.6	7.26	12.9	13.4	2.55	0.85	0.45
May 20	1830	10.0	83.8	430	2.6	6.54	14.0	13.2	3.30	1.37	0.81
May 20	1930	10.3	84.3	420	2.4	6.07	13.8	13.2	3.71	1.73	1.11
May 20	2030	9.8	86.8	360	2.1	6.54	15.9	14.2	4.02	1.63	0.95
May 20	2130	10.1	87.7	377	1.9	6.07	14.9	13.2	3.34	1.22	0.67
May 20	2230	9.5	87.6	397	2.7	6.82	13.6	12.8	3.52	1.42	0.83
May 20	2330	9.2	87.6	400	2.7	6.15	12.9	12.7	3.46	1.46	0.89
May 21	30	9.6	87.3	420	3.0	6.14	13.1	11.8	2.58	9.93	0.56
May 21	130	9.2	88.3	490	2.0	5.69	13.5	12.9	3.33	1.26	0.71
May 21	230	8.8	87.4	520	1.7	5.29	13.3	13.4	3.44	1.39	0.81
May 21	330	8.2	86.1	560	2.7	6.11	11.8	10.9	2.18	0.73	0.39
May 21	430	8.5	83.1	597	2.2	5.55	11.6	97.1	1.78	0.65	0.36
May 21	530	8.2	81.3	620	2.0	5.33	10.9	97.5	1.85	0.73	0.43
May 21	630	7.9	79.7	680	1.8	5.02	11.1	10.7	1.96	0.67	0.36

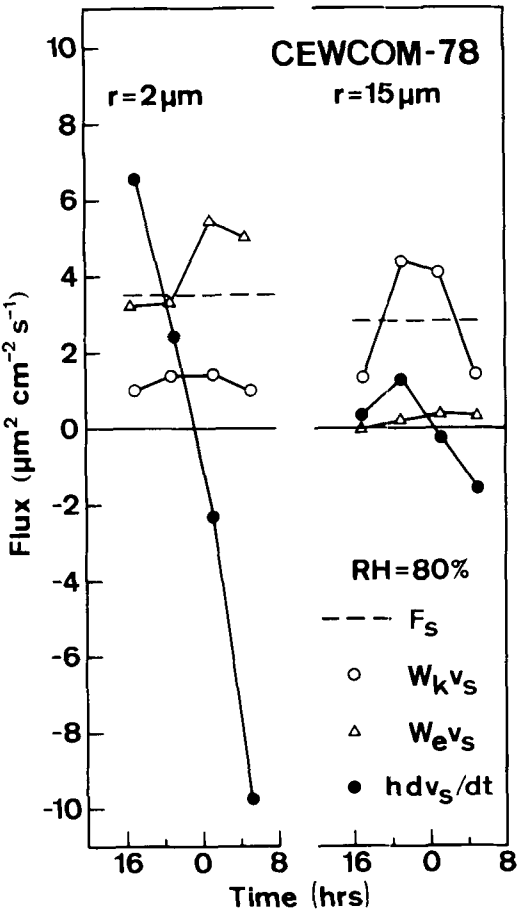

Fig. 3. Time series of the terms of eq. (9) for 2 μm radius and 15 μm radius particles. The dashed line is the average contribution of the surface production term and should be the sum of the other three terms.

tion flux spectrum is shown in Fig. 4. This flux spectrum applies to the average surface conditions for the entire 20 h period (average wind speed was about 9 m s^{-1}). The error bars represent the uncertainty in the mean estimate.

The relative contributions of entrainment, gravitational fallout and surface production are nicely illustrated by defining an equivalent surface production vertical velocity, $W_F = F_s/v_s$ so that in equilibrium ($dv_s/dt = 0$).

$$W_F = W_e + W_k \tag{10}$$

For the average conditions found in the analysis period, the entrainment and Stokes terms were roughly equal at a particle radius of 5 μm (Fig. 5). Thus, at a radius of 5 μm the density of sea salt particles in the mixed layer is being reduced about as effectively by entrainment (dilution of mixed layer air with air from above the inversion) as it is by gravitational fallout. Hence the neglect of the entrainment process in aerosol dynamics can lead to serious errors.

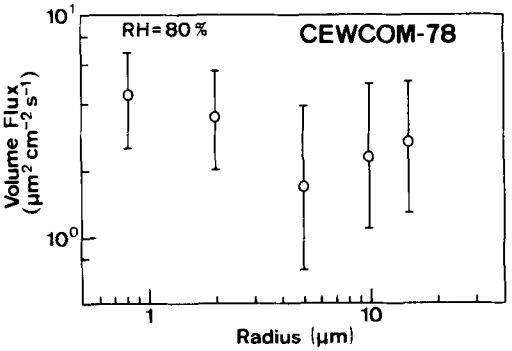

Fig. 4. The ensemble average surface flux spectrum, $F_s(r)$, for the CEWCOM-78 analysis period (average wind speed, 9 m s^{-1}).

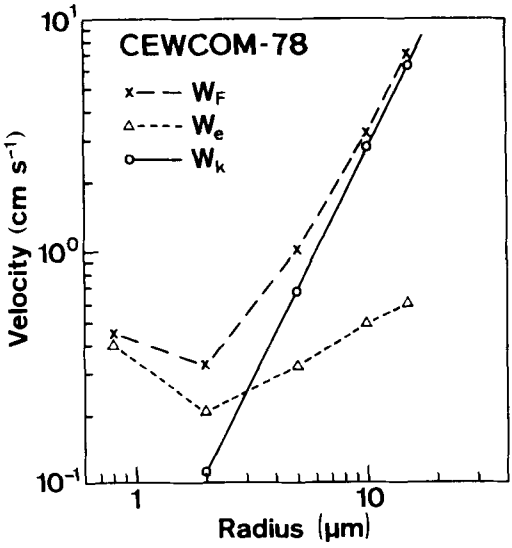

Fig. 5. Ensemble average contribution of entrainment (W_e), Stokes fallout (W_k) and surface flux ($W_F = F_s/v_s$) assuming a state of dynamic equilibrium.

4. Flux spectrum and wind speed

Because of the reasonably constant wind speeds during the 20 h CEWCOM-78 period, we were able to improve the statistical certainty for the $\bar{F}_s$ calculation by combining all the data from the period, assuming that the flux would be a reasonable representation for $U = 9$ m s^{-1} wind speed. Thus, we now have the surface flux spectrum at a single wind speed. In order to estimate the flux at

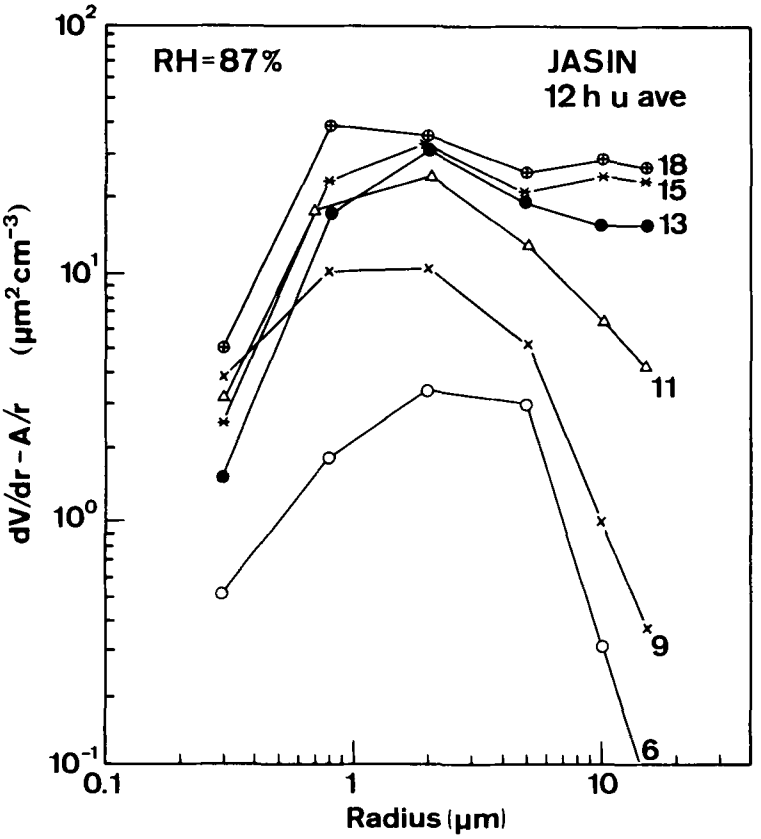

Fig. 6. Ensemble average equilibrium sea salt volume spectra from JASIN. The number to the right of the spectrum is the wind speed category in m s^{-1}.

Table 2. *Equilibrium sea-salt aerosol spectra in* $\mu m^2\ cm^{-3}$ *as a function of radius* (μm) *and wind speed* ($m\ s^{-1}$)

↓ u	$r \rightarrow$ 0.8	2	5	10	15
6	2.8	3.4	3	0.3	0.05
9	10	10	5	1	0.35
11	18	25	13	6.4	4.2
13	20	30	20	15	15
15	24	33	22	22	22
18	28	35	28	28	28
9*	9	11	2	0.8	0.4

* CEWCOM-78 analysis period.

other wind speeds, we note that the right-hand side of eq. (10) is nearly independent of wind speed for equilibrium conditions. Although the maximum of the equilibrium spectrum does shift to larger radii with increasing wind speed, this is due to increased production of salt particles by the ocean. The Stokes velocity is explicitly calculated from eq. (8a)

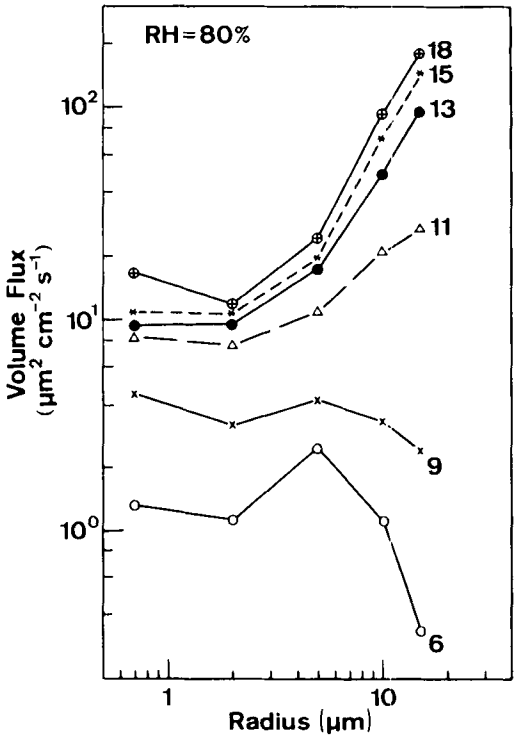

Fig. 7. Ensemble average surface flux spectra deduced from eq. (11) and Table 2. The number to the right of the spectrum is the wind speed in m s^{-1}.

and contains no wind speed dependence. The entrainment velocity, W_e, probably has only a weak dependence on wind speed. Therefore, the flux at one wind speed can be related to the flux at other wind speeds if the equilibrium volume spectra are known:

$$F_s(U_1) = F_s(U_2)v_s(U_1)/v_s(U_2) \tag{11}$$

We have available from JASIN a large set of ensemble averages of aerosol volume spectra at different wind speeds (Fig. 6 and Table 2). It is a simple matter to apply this data to eq. (11), using the CEWCOM-78 aerosol flux and equilibrium spectrum to generate the surface volume flux spectra as a function of wind speed (Fig. 7 and Table 3). At a wind speed of 6.0 m s^{-1}, the flux can be integrated in radius space to yield a total sea-salt dry mass production rate of 4.8 mg m^{-2} day^{-1} which compares well with the 4.4 mg m^{-2} day^{-1} estimated by Blanchard (1963) and 4.2 mg m^{-2} day^{-1} estimated by Kritz and Rancher (1980).

5. Non-equilibrium

For time periods of a few hours, the aerosol spectrum may not be in a state of dynamic equilibrium. If we rewrite eq. (7) in the following form:

$$dv_s/dt + v_s/\tau_p = F_s/h \tag{12}$$

where the time constant, τ_p, is

$$\tau_p = h/(W_e + W_k) \tag{13}$$

then we see the analogy of aerosols and a capacitor charged by an applied "voltage" F_s. through a

Table 3. *Surface sea-salt aerosol flux, $F_s(r)$, (μm^2 cm^{-2} s^{-1}) as a function of particle radius (μm) and wind speed ($m\ s^{-1}$)*

↓ u	$r \rightarrow$0.8	2	5	10	15
6	1.3	1.1	2.5	1.0	0.33
9	4.5	3.1	4.2	3.3	2.3
11	8.2	7.7	11	21	27
13	9.1	9.2	17	49	48
15	11	10	19	72	140
18	17	11	24	92	180
9*	4.1	3.4	1.7	2.3	2.6

* CEWCOM-78 analysis period.

"resistance" $(W_e + W_k)^{-1}$ where the "capacitance" is h.

The response time of the aerosol density is a strong function of particle radius because $W_k \sim r^2$. Values of τ_p for $S = 0.8$ and $h = 400$ m are given in Table 4.

The boundary layer mixing time, τ_m, which represents the time required for changes in aerosol density to be evenly distributed throughout the marine layer is:

$$\tau_m = h/W_* \tag{14}$$

For the CEWCOM-78 analysis period ($h = 400$ m and $W_* = 0.6$ m s^{-1}) we find $\tau_m = 0.19$ h. Therefore, short term variations in mixing volume (dh/dt) will lead to changes in the aerosol density because the production response time is much slower than the mixing time. Thus, for time periods of the order of one hour, changes in the aerosol density ($h\, dv_s/dt$) will be highly correlated with the mixing volume term ($v_s\, dh/dt$). This effect, which is particularly noticeable for smaller particles (see Fig. 3 and Table 3), is shown in Fig. 8.

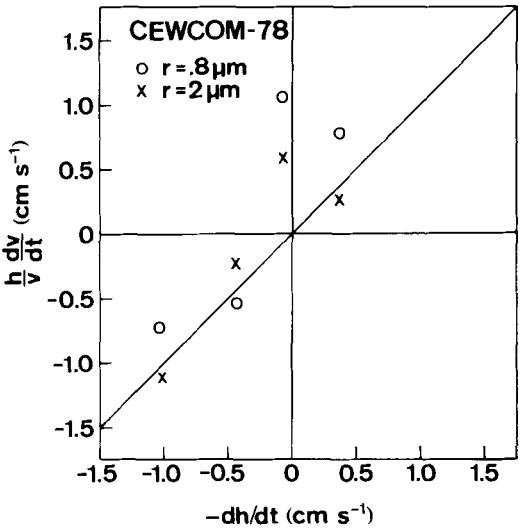

Fig. 8. Changes in aerosol spectral density (dv_s/dt) versus changes in mixing volume (dh/dt). This graph illustrates the dominance of these terms in eq. (9) for short time periods.

Table 4. *The equilibrium time constant for aerosols at $S = 0.8$, $h = 400$ m and $W_e = 0.4$ cm s^{-1}*

r (μm)	0.5	1	5	10	15
τ_p (hours)	28	22	11	3.5	0.5

6. Acknowledgements

This work was supported by the Naval Material Command (EO/MET) and the Naval Air Systems Command (Air 370).

REFERENCES

Barnhardt, E. A. and Streete, J. L. 1970. A method for predicting atmospheric aerosol scattering coefficients in the infrared. *Appl. Opt. 9*, 1337–1334.

Blanchard, D. C. and Woodcock, A. U. 1957. Bubble formation and modification in the sea and its meteorological significance. *Tellus 9*, 145–157.

Blanchard, D. C. 1963. Electrification of the atmosphere by particles from bubbles in the sea. *Progr. Oceanogr. 1*, 72–202.

Fairall, C. W., Davidson, K. L., and Schacher, G. E. 1982. Application of a mixed layer model to aerosols in the coastal marine boundary layer, Proc. First Int. Conf. on Meteorology and Air/Sea Interaction in the Coastal Zone, AMS, Boston.

Deardorff, J. W. 1976. On the entrainment rate of a stratocumulus-topped mixed layer. *Quart J.R. Met. Soc. 102*, 563–582.

Fitzgerald, J. W. 1975. Approximation formulas for the equilibrium size of an aerosol particle as a function of its dry size and composition and the ambient relative humidity. *J. Appl. Meteor. 14*, 1044–1049.

Hughes, H. G. and Richter, J. H. 1980. Extinction coefficients calculated from aerosol size distributions measured in a marine environment. *Opt. Engin. 19*, 616–620.

Kaimal, J. C., Wyngaard, J. C., Haugen, D., Cote, O. R. and Izumi, Y. 1976. Turbulence structure in the convective boundary layer. *J. Atmos. Sci. 33*, 2152–2169.

Kritz, M. A. and Rancher, J. 1980. Circulation of Na, Cl, and Br in the tropical marine atmosphere. *J. Geophys. Res. 85*, 1633–1639.

Larsen, R. E., Kasemir, W. and Bressan, D. J. 1979. Measurements of atmospheric ^{222}Rn at San Nicolas Island and over nearby California coastal areas during CEWCOM-78. Naval Research Laboratory, Washington, D.C., Technical Report 3941, 13 pages.

Markson, R., Sedlacek, J. and Fairall, C. W. 1981. Turbulent transport of electric charge in the marine atmospheric boundary layer. *J. Geophys. Res. 86*, 12115–12121.

Monahan, E. C., Davidson, K. L. and Spiel, D. E. 1982. Whitecap aerosol productivity deduced from simulation tank measurements. *J. Geophys. Res.* (to appear).

Schacher, G. E., Davidson, K. L., Fairall, C. W. and Spiel, D. E. 1981. Calculation of optical extinction from aerosol spectral data. *Appl. Opt. 20*, 3951–3957.

Wu, J. 1979. Spray in the atmospheric surface layer: review and analysis of laboratory and oceanic results. *J. Geophys. Res. 84*, 1693–1704.